

Direct infrared observation of hydrogen chloride anions in solid argon

Cite as: J. Chem. Phys. **147**, 114301 (2017); <https://doi.org/10.1063/1.4993638>

Submitted: 29 June 2017 . Accepted: 31 August 2017 . Published Online: 18 September 2017

Tzu-Ping Huang, Hui-Fen Chen, Meng-Chen Liu, Chih-Hao Chin, Marcus C. Durrant, Yin-Yu Lee, and Yu-Jong Wu



View Online



Export Citation



CrossMark

ARTICLES YOU MAY BE INTERESTED IN

[Near-infrared spectroscopy and anharmonic theory of the \$\text{H}_2\text{O}^+ \text{Ar}_{1,2}\$ cation complexes](#)

The Journal of Chemical Physics **147**, 104302 (2017); <https://doi.org/10.1063/1.4998419>

[Spectroscopic properties of photosystem II reaction center revisited](#)

The Journal of Chemical Physics **147**, 115102 (2017); <https://doi.org/10.1063/1.4997527>

[Communication: The \$\text{Al} + \text{CO}_2 \rightarrow \text{AlO} + \text{CO}\$ reaction: Experiment vs. theory](#)

The Journal of Chemical Physics **147**, 171101 (2017); <https://doi.org/10.1063/1.5007874>

PHYSICS TODAY

WHITEPAPERS

ADVANCED LIGHT CURE ADHESIVES

Take a closer look at what these environmentally friendly adhesive systems can do

READ NOW

PRESENTED BY
MASTERBOND
ADHESIVES | SEALANTS | COATINGS



Direct infrared observation of hydrogen chloride anions in solid argon

Tzu-Ping Huang,¹ Hui-Fen Chen,² Meng-Chen Liu,¹ Chih-Hao Chin,¹ Marcus C. Durrant,³ Yin-Yu Lee,¹ and Yu-Jong Wu^{1,4,a}

¹National Synchrotron Radiation Research Center, 101 Hsin-Ann Road, Hsinchu Science Park, Hsinchu 30076, Taiwan

²Department of Medicinal and Applied Chemistry, Kaohsiung Medical University, 100, Shih-Chuan 1st Road, Kaohsiung 80708, Taiwan

³Department of Applied Sciences, Northumbria University, Newcastle upon Tyne NE1 8ST, United Kingdom

⁴Department of Applied Chemistry, National Chiao Tung University, 1001, Ta-Hsueh Road, Hsinchu 30010, Taiwan

(Received 29 June 2017; accepted 31 August 2017; published online 18 September 2017)

To facilitate direct spectroscopic observation of hydrogen chloride anions (HCl^-), electron bombardment of CH_3Cl diluted in excess Ar during matrix deposition was used to generate this anion. Subsequent characterization were performed by IR spectroscopy and quantum chemical calculations. Moreover the band intensity of HCl^- decays slowly when the matrix sample is maintained in the dark for a prolonged time. High-level *ab initio* calculation suggested that HCl^- is only weakly bound. Atom-in-molecule charge analysis indicated that both atoms of HCl^- are negatively charged and the Cl atom is hypervalent. *Published by AIP Publishing.* [<http://dx.doi.org/10.1063/1.4993638>]

I. INTRODUCTION

The hydrogen chloride anion (HCl^-) has received much attention because it serves as a model system for investigating the electronic structures of anions and the related processes of electron dissociative attachment and associative attachment.^{1–10} Early experimental observation of HCl^- was achieved via low-energy electron collision processes in HCl, and a regular spacing of ~ 0.3 eV was detected for Cl^- anions obtained through dissociative attachment;^{1–3} this regular spacing was believed to correspond to the vibrational structure of the low-lying state of HCl^- . Later, detection of HCl^- signals in solid matrices was achieved using an electron paramagnetic resonance method.^{11,12} Moreover, the charge-separated species $\text{Xe}^+(\text{HCl})^-$ was prepared in a Xe matrix.¹³ Because neutral HCl is more stable than the corresponding anion, HCl^- has an autodetachment lifetime and metastable states.^{1–10,14,15} Calculation of the metastable behavior of the electronic states associated with resonance wavefunctions remains a challenge to theoretical chemists, particularly in the HCl^- system. The potential curve of the HCl^- ground state parallels that of its neutral form HCl in the region around the minimum, but curve crossing occurs at a large nuclear distance, which results in the most stable anionic state ($1\ ^2\Sigma^+$) being located below the neutral ground state ($X\ ^1\Sigma^+$). Further calculations have shown that most HCl^- potentials are parallel and above the ground-state potential curve of HCl, which makes these corresponding states similar to a discrete representation of a continuum.^{5–10} Recently, Honigmann *et al.* reported detailed information about the metastable electronic states of HCl^- by using the complex multireference single- and double-excitation configuration interaction (MRD-CI) method.¹⁶ They concluded that the $1\ ^2\Sigma^+$ state of HCl^- is a bound anionic

ground state that is responsible for the sharp peak observed in the low-energy region of electron-scattering experiments. In contrast, the broad resonance band at 2.6 eV is caused by the upper $3\ ^2\Sigma^+$ state of HCl^- with a larger bond length.

In our previous work,¹⁷ we produced and trapped hydrogen fluoride anions (HF^-) in a solid Ar matrix; these anions were generated by electron bombardment of an Ar matrix containing a small amount of CH_3F during deposition and were identified by observing the ro-vibrational bands of the HF stretching mode. The calculated valence electron equivalent (γ), which describes the effective number of valence electrons on any particular atom based on an analysis of the atomic charges in the molecule,¹⁸ indicated that the F atom of this anion is hypervalent. Moreover, this anion was only observed by electron bombardment of a $\text{CH}_3\text{F}/\text{Ar}$ sample with higher bombardment energy suggested that the formation of HF^- resulted from the association reaction of H with F^- . Irradiation with the selected wavelength increased amounts of HF^- owing to increased mobility and combination of H atoms and F^- anions in the solid matrix. Trapping this anion in a solid matrix might increase the energy threshold for electron detachment,^{19,20} providing sufficient stability for optical detection of HF^- . In this work, we extended our study to IR identification of HCl^- . To the best of our knowledge, direct spectroscopic observation of this anion has not been reported. By using a similar method, we recorded the IR spectrum of HCl^- anions produced in an argon matrix. High-level *ab initio* calculations on spectroscopic parameters of the ground state ($X\ ^2\Sigma^+$) HCl^- were performed to support our experimental observations.

II. EXPERIMENTS AND THEORETICAL METHODS

The experimental setup has been described previously.^{17,21,22} IR absorption spectra covering the spectral range

^aE-mail: yjw@nsrc.org.tw

of 450–5000 cm^{-1} were recorded with an interferometric spectrometer (Bruker v80) equipped with a KBr beam splitter and a Hg–Cd–Te detector cooled to 77 K. Typically, 400 scans at a resolution of 0.25 cm^{-1} were recorded at each stage of the experiment.

The anions were produced by electron bombardment of a gaseous sample containing a small proportion of CH_3Cl during the deposition of an Ar matrix. An electron beam at 1500 eV with a current of 300 μA was generated with an electron gun (Kimball Physics, Model EFG-7). Typically, a gaseous mixture of $\text{CH}_3\text{Cl}/\text{Ar}$ (1/500) was deposited over a period of 4 h with a flow rate of 5–8 mmol h^{-1} . Experiments with CH_4/Ar (1/500), $\text{CD}_3\text{Cl}/\text{Ar}$ (1/500), $^{13}\text{CH}_3\text{Cl}/\text{Ar}$ (1/500), $\text{CD}_3\text{Cl}/\text{CH}_3\text{Cl}/\text{Ar}$ (1.5/1/1000), and Ar were conducted using the same conditions. Photoirradiation experiments were performed with synchrotron radiation at BL03 of Taiwan light source (~ 5 mW at 210 nm) and light-emitting diodes (bandwidth ~ 10 nm, 350 mW at 450 nm, 170 mW at 520 and 625 nm). Ar (99.9999%, Scott Specialty Gases), CH_3Cl (99.5%, Matheson), $^{13}\text{CH}_3\text{Cl}$ ($\sim 99\%$ ^{13}C , Aldrich), and CD_3Cl ($\sim 99\%$ deuterium, Aldrich) were used without further purification, except for a freeze–pump–thaw procedure at 77 K.

The energies, equilibrium structures, vibrational wavenumbers, and IR intensities of the species were calculated using the Gaussian 09 program.²³ The spectroscopic parameters of HCl^- were calculated at the CCSD(T) level of theory^{24,25} with the aug-cc-pVQZ basis set.²⁶ The charge distribution of the species was calculated with the AIMAll program.²⁷

III. RESULTS AND DISCUSSION

Figures 1(A)–1(C) depict partial IR spectra of electron-bombarded $\text{CH}_3\text{Cl}/\text{Ar}$ (1/500), CH_4/Ar (1/500), and pure Ar samples, respectively, under the same experimental conditions. Comparison of these spectra clearly shows that the triplet feature at 2454.5, 2438.3, and 2419.3 cm^{-1} is only obtained for the electron-bombarded $\text{CH}_3\text{Cl}/\text{Ar}$ matrix sample. Moreover, the observation of rotational parameters (~ 8.8 cm^{-1})

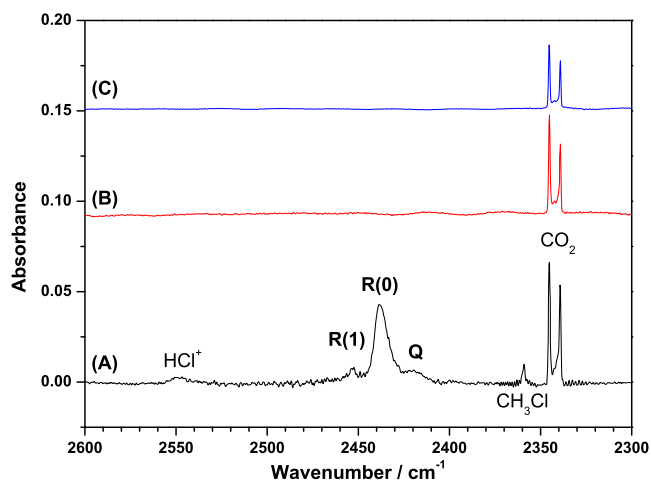


FIG. 1. Partial IR spectra of electron-bombarded (1500 eV, 0.3 mA) matrix samples at 10 K. (A) $\text{CH}_3\text{Cl}/\text{Ar}$ (1/500), (B) CH_4/Ar (1/500), and (C) Ar. The ro-vibrational transitions of the HCl^- bands and the other observed bands are assigned.

similar to that of HCl^{28} indicates that the carrier is a simple hydride species. As the vibrational frequencies of C–H and C–Cl stretching modes are typically beyond this spectral region, the observed broad features may arise from the overlapping bands of $^{35,37}\text{Cl}$ -isotopic variants, suggesting that this triplet feature is associated with the H–Cl stretching mode. Table S1 in the [supplementary material](#) lists the assignments of all observed peaks in this experiment and the reaction mechanisms and band assignments of other species will be discussed elsewhere.

For further confirmation of the spectral assignments of HCl^- , electron bombardment of $^{13}\text{CH}_3\text{Cl}/\text{Ar}$ (1/500) and $\text{CD}_3\text{Cl}/\text{Ar}$ (1/500) matrix samples was performed using experimental procedures similar to those for $\text{CH}_3\text{Cl}/\text{Ar}$. As shown in Figs. 2(A) and 2(B) for $\text{CH}_3\text{Cl}/\text{Ar}$ and $^{13}\text{CH}_3\text{Cl}/\text{Ar}$, respectively, the positions of the observed features are identical, indicating that the carrier contains no carbon atoms. Figure 2(C) shows that deuterium isotopic substitution shifts the triplet band to 1782.6 and 1770.2 cm^{-1} ; the R(1) feature, which is absent from this spectrum, might be buried in the strong R(0) band. The observed deuterium isotopic shift ratio of 0.731 is comparable to those of HCl (0.724) and HCl^+ (0.726),¹⁹ which is consistent with the assignment of this feature as HCl^- . In addition, an experiment was performed using a mixed isotopic sample $\text{CH}_3\text{Cl}/\text{CD}_3\text{Cl}/\text{Ar}$ (1/1.5/1000); the corresponding IR spectra are shown in Fig. S1 of the [supplementary material](#). No additional features were observed in the mixed isotopic experiment, suggesting that this carrier contains only one H atom. Furthermore, identification of the H–Cl stretch of HCl^+ at 2548.4 cm^{-1} in solid Ar¹⁹ excludes the possibility that this new IR feature is associated with HCl^+ . Therefore, the above evidence supports that the carrier corresponding to the triplet feature is HCl^- .

We performed quantum-chemical calculations using the CCSD(T) method with the aug-cc-pVQZ basis set to locate the stable structure of HCl^- . The bond length was predicted to be 1.307 Å, as compared with 1.284 Å predicted previously by Honigmann *et al.* using MRD-CI.¹⁶ The intense band of HCl^- observed at 2438.3 cm^{-1} fits well with the harmonic vibrational wavenumber of 2498 cm^{-1} predicted by

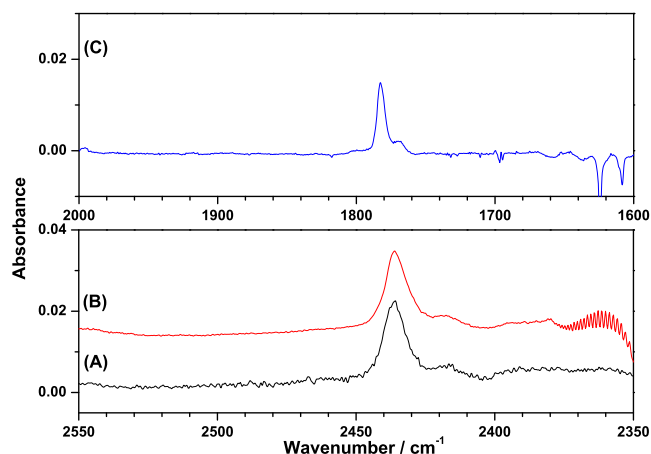


FIG. 2. IR spectra of the electron-bombarded matrix samples of (A) $\text{CH}_3\text{Cl}/\text{Ar}$ (1/500), (B) $^{13}\text{CH}_3\text{Cl}/\text{Ar}$ (1/500), and (C) $\text{CD}_3\text{Cl}/\text{Ar}$ (1/500) at 10 K.

the CCSD(T) method and also fits well with the anharmonic value of 2473.5 cm^{-1} predicted by the MRD-CI method.¹⁶ In addition, the rotational constant of HCl^- was predicted to be 10.0 cm^{-1} by CCSD(T), which is consistent with the value of 10.4 cm^{-1} predicted by MRD-CI (Ref. 16) and the experimental value of 8.8 cm^{-1} . Table S2 of the [supplementary material](#) compares the results predicted by a CCSD(T) method with various basis sets. For DCl^- , the vibrational wavenumber of 1792 cm^{-1} and the rotational constant of 5.2 cm^{-1} predicted by CCSD(T) are also in good agreement with our experimental values of 1782.6 cm^{-1} and 6.2 cm^{-1} , respectively. Moreover, the calculated band splitting between H^{35}Cl^- and H^{37}Cl^- is less than 1.4 cm^{-1} , which is consistent with the observation of a bandwidth of about 7 cm^{-1} for the R(0) band, as shown in Fig. 2. Taken together, the satisfactory agreement between theoretical predictions and experimental observations further supports our assignment of this spectral feature as HCl^- . Although the observed spacing of the triplet peaks of HCl^- is consistent with the theoretical prediction and the rotational constant of HCl , we cannot completely exclude these possibilities for the sidebands from libration or phonon coupling.

To further check the stability of this anion, we maintained the matrix sample in the dark for 12 h and found little decay of the HCl^- band intensity, as shown in Fig. 3(A). In these difference spectra, lines pointing upward indicate the production of species, whereas those pointing downward indicate the destruction of species. We also performed secondary photolysis of HCl^- at various wavelengths to study the related photochemical behavior. Because a shallow minimum is predicted for the ground state of HCl^- by the previous work¹⁶ and ours shown in Fig. 4, photodetachment and/or photodissociation of this anion should be possible in the near-IR and visible regions. We found that irradiation at 210, 520, and 625 nm for 1 h depleted this anion, as shown in Fig. 3, but no change in the band intensity was found upon irradiation with IR light provided by a global source for 4 h.

It is worth noting that in our previous work, irradiation of the electron-bombarded matrix sample ($\text{CH}_3\text{F}/\text{Ar}$) at 210 nm

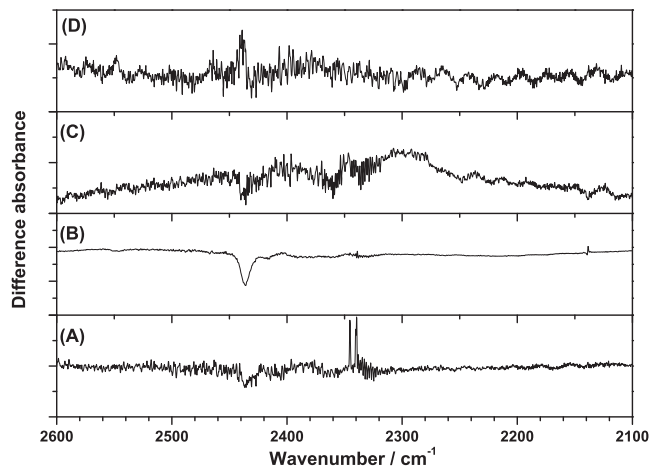


FIG. 3. Difference IR spectra of the electron-bombarded $\text{CH}_3\text{Cl}/\text{Ar}$ (1:500) (A) sitting in the dark for 12 h, (B) upon irradiation at 210 nm for 1 h, (C) upon irradiation at 625 nm for 1 h, and (D) upon irradiation at 450 nm for 1 h. All spectra were recorded in separate experiments.

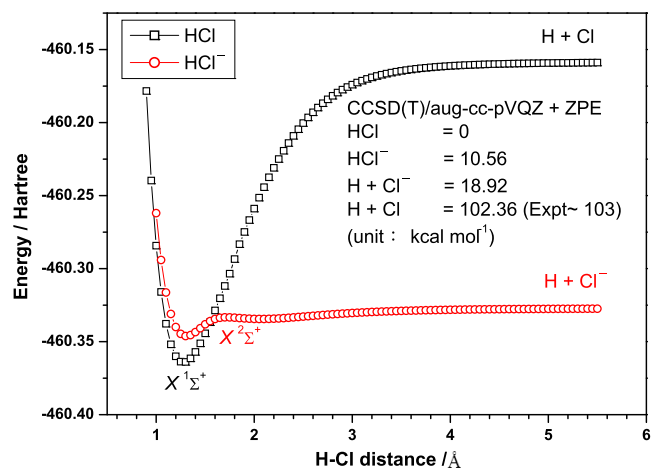


FIG. 4. Potential energy surfaces of neutral and anionic HCl in their ground states, calculated at a CCSD(T)/aug-cc-pVQZ level of theory. The energy difference between the two species is listed with zero-point energy correction.

enhanced the formation of HF^- efficiently.¹⁷ However, in the present study, the amount of HCl^- increased somewhat upon irradiation of the matrix sample ($\text{CH}_3\text{Cl}/\text{Ar}$) at 450 nm, as shown in Fig. 3(D). This observed difference may result from the different dissociation energies (D_0) of these species. D_0 of HF^- is predicted to be 182.1 kJ mol^{-1} , which is comparable to the bond strength of a typical halogen-halogen bond. By contrast, D_0 of HCl^- is only 34.3 kJ mol^{-1} , as shown in Fig. 4, and hence the photoinduced combination of H and Cl^- to form HCl^- with excess energy might lead to the reverse reaction.

The charge distribution of HCl^- was calculated by the atom-in-molecule (AIM) method,¹⁸ as shown in Fig. S2 of the [supplementary material](#). Both the chlorine and hydrogen atoms were found to possess negative charges, and the H atom showed hydride character. The calculated valence electron equivalent (γ) was 8.22e for the Cl atom and 2.00e for the H atom, suggesting that the Cl atom in HCl^- is hypervalent. Therefore, HCl^- is clearly a hypervalent species.

IV. CONCLUSION

In summary, HCl^- was produced by electron bombardment of an Ar matrix containing a small amount of CH_3Cl during deposition, and its ro-vibrational features were assigned and compared with those obtained by theoretical calculations. Irradiation of the matrix sample at 210, 520, and 625 nm depleted HCl^- , whereas no change was observed upon irradiation with an IR global source. In addition, irradiation at 450 nm increased the amount of HCl^- somewhat owing to the photoinduced combination of H atoms and Cl^- anions in the matrix. The calculated charge distribution for HCl^- indicated that both the chlorine and hydrogen atoms possess negative charges. Moreover, the H atom exhibited hydride character and the Cl atom was hypervalent, indicating that HCl^- is a hypervalent species. This study providing the direct spectroscopic measurement of HCl^- is useful for theorists in dealing with the problems of predictions of the resonance states.

SUPPLEMENTARY MATERIAL

See [supplementary material](#) for difference IR spectra of HCl^- anions in a mixed isotopic sample in an Ar matrix irradiated with 210 nm and the calculation of spectroscopic parameters at CCSD(T) with various basis sets, and the valence electron equivalent (γ).

ACKNOWLEDGMENTS

This work was supported by the Ministry of Science and Technology of the Republic of China (Grant Nos. MOST105-2113-M-213-001 and 106-2113-M-213 -002 -MY3) and the National Synchrotron Radiation Research Center.

¹J. P. Ziesel, I. Nenner, and G. J. Schulz, *J. Chem. Phys.* **63**, 1943 (1975).

²G. E. Caledonia and R. E. Center, *J. Chem. Phys.* **64**, 4237 (1976).

³K. Rohr and F. Linder, *J. Phys. B: At. Mol. Phys.* **9**, 2521 (1976).

⁴M. Rajzmann, F. Spiegelmann, and J. P. Malrieu, *J. Chem. Phys.* **89**, 433 (1988).

⁵F. Figuet-Fayard, *J. Phys. B: At. Mol. Phys.* **7**, 810 (1974).

⁶M. Bettendorff, R. J. Buenker, and S. D. Peyerimhoff, *Mol. Phys.* **50**, 1363 (1983).

⁷S. V. O'Neil, P. Rosmus, D. W. Norcross, and H.-J. Werner, *J. Chem. Phys.* **85**, 7232 (1986).

⁸H. S. Taylor, E. Goldstein, and G. A. Segal, *J. Phys. B: At. Mol. Phys.* **10**, 2253 (1977).

⁹E. Goldstein, G. A. Segal, and R. W. Wetmore, *J. Chem. Phys.* **68**, 271 (1978).

¹⁰M. Čížek, J. Horáček, and W. Domcke, *Phys. Rev. A* **60**, 2873 (1999).

¹¹D. M. Lindsay, M. C. R. Symons, D. R. Herschbach, and A. L. Kwiram, *J. Phys. Chem.* **86**, 3789 (1982).

¹²J. B. Raynor, I. J. Rowland, and M. C. R. Symons, *J. Chem. Soc., Dalton Trans.* **1987**, 421.

¹³M. E. Fajardo and V. A. Apkarian, *J. Chem. Phys.* **85**, 5660 (1986).

¹⁴C. J. Howard, F. C. Fehsenfeld, and M. McFarland, *J. Chem. Phys.* **60**, 5086 (1974).

¹⁵T. S. Zwier, M. M. Maricq, C. J. S. M. Simpson, V. M. Bierbaum, G. B. Ellison, and S. R. Leone, *Phys. Rev. Lett.* **44**, 1050 (1980).

¹⁶M. Honigmann, H.-P. Liebermann, and R. J. Buenker, *J. Chem. Phys.* **133**, 044305 (2010).

¹⁷M.-C. Liu, H.-F. Chen, C.-H. Chin, T.-P. Huang, Y.-J. Chen, and Y.-J. Wu, *Sci. Rep.* **7**, 2984 (2017).

¹⁸M. C. Durrant, *Chem. Sci.* **6**, 6614 (2015).

¹⁹D. Forney, M. E. Jacox, and W. E. Thompson, *J. Chem. Phys.* **103**, 1755 (1995).

²⁰W. E. Thompson and M. E. Jacox, *J. Chem. Phys.* **111**, 4487 (1999).

²¹M.-C. Liu, S.-C. Chen, C.-H. Chin, T.-P. Huang, H.-F. Chen, and Y.-J. Wu, *J. Phys. Chem. Lett.* **6**, 3185 (2015).

²²M.-C. Liu, H.-F. Chen, W.-J. Huang, C.-H. Chin, S.-C. Chen, T.-P. Huang, and Y.-J. Wu, *J. Chem. Phys.* **145**, 074314 (2016).

²³M. J. Frisch *et al.*, GAUSSIAN 09, Revision A.02, Gaussian, Inc., Wallingford, CT, USA, 2009.

²⁴J. D. Watts, J. Gauss, and R. J. Bartlett, *J. Chem. Phys.* **98**, 8718 (1993).

²⁵J. A. Pople, M. Head-Gordon, and K. Raghavachari, *J. Chem. Phys.* **87**, 5968 (1987).

²⁶D. E. Woon and T. H. Dunning, Jr., *J. Chem. Phys.* **98**, 1358 (1993).

²⁷T. A. Keith, AIMAll, version 17.01.25, TK Gristmill Software, Overland Park, KS, USA, 2017, aim.tkgristmill.com.

²⁸C. P. Rinsland, M. A. H. Smith, A. Goldman, V. M. Devi, and D. C. Benner, *J. Mol. Spectrosc.* **159**, 274 (1993).